blood

Prepublished online August 1, 2012;
doi:10.1182/blood-2012-02-408252

Induction of IL-4Rα-dependent microRNAs identifies PI3K/Akt signaling as essential for IL-4-driven murine macrophage proliferation *in vivo*

Dominik Rückerl, Stephen J. Jenkins, Nouf N. Laqtom, Iain J. Gallagher, Tara E. Sutherland, Sheelagh Duncan, Amy H. Buck and Judith E. Allen

Blood (print ISSN 0006-4971, online ISSN 1528-0020), is published weekly by the American Society of Hematology, 2021 L St, NW, Suite 900, Washington DC 20036.

Induction of IL-4Rα-dependent microRNAs identifies PI3K/Akt signaling as essential for IL-4-driven murine macrophage proliferation *in vivo*

short title: microRNAs and control of proliferation in AAMΦ

Dominik Rückerl[1], Stephen J. Jenkins[1], Nouf N. Laqtom[1,2], Iain J. Gallagher[3], Tara E. Sutherland[1], Sheelagh Duncan[1], Amy H. Buck[1] and Judith E. Allen[1]

[1]Institute of Immunology and Infection Research, Centre for Immunity, Infection and Evolution, School of Biological Sciences, University of Edinburgh, Edinburgh, United Kingdom; [2]Department of Biology, King Abdulaziz University, Jeddah, Saudi Arabia; [3]Medical Research Council Centre for Regenerative Medicine, University of Edinburgh, Edinburgh, United Kingdom

Corresponding author: Judith E. Allen, Institute of Immunology and Infection Research, Centre for Immunity, Infection and Evolution, University of Edinburgh, Ashworth Laboratories, West Mains Road, EH9 3JT Edinburgh, UK; phone: +44-(0)131-6507014; Fax: +44-(0)131-6505450; email: j.allen@ed.ac.uk

Category: PHAGOCYTES, GRANULOCYTES AND MYELOPOIESIS

Abstract:

Macrophage (MΦ) activation must be tightly controlled to preclude overzealous responses that cause self-damage. MicroRNAs have been shown to promote classical MΦ activation by blocking anti-inflammatory signals and transcription factors, but can also prevent excessive TLR-signaling. In contrast, the microRNA profile associated with alternatively activated MΦ and their role in regulating wound-healing or anti-helminthic responses has not been described. Utilizing an *in vivo* model of alternative activation, in which adult *Brugia malayi* nematodes are surgically implanted in the peritoneal cavity of mice, we identified differential expression of miR-125b-5p, miR-146a-5p, miR-199b-5p and miR-378-3p in helminth induced MΦ. *In vitro* experiments demonstrated that miR-378-3p was specifically induced by IL-4 and revealed the IL-4-Receptor/PI3K/Akt-signaling pathway as a target. Chemical inhibition of this pathway showed that intact Akt-signaling is an important enhancement factor for alternative activation *in vitro* and *in vivo* and is essential for IL-4 driven MΦ proliferation *in vivo*. Thus our identification of miR-378-3p as an IL-4Rα-induced microRNA, led to the discovery that Akt regulates the newly discovered mechanisms of IL-4 driven macrophage proliferation. Together the data suggest that negative regulation of Akt-signaling via microRNAs might play a central role in limiting MΦ expansion and alternative activation during type 2 inflammatory settings.

Introduction

Macrophages (MΦ) are centrally involved in recognising and containing pathogens. Subsequently they ensure the efficient induction and upkeep of a protective adaptive immune response. MΦ also help to limit the ensuing immune reaction as well as clear apoptotic cells and other debris.[1] The adaption of MΦ to these diverse roles is reflected in the multitude of activation phenotypes that have been described.[2] Classical (or M1-) and IL-4Rα-driven alternative (or M2-) activation represent the two most divergent phenotypes with the former thought to be proinflammatory and important for the clearance of microbial pathogens, whereas the latter are predominantly found during helminth-infections and are associated with wound-healing and immuno-suppression.[3-6] In either case, MΦ-activation must be tightly controlled, as excessive activation can lead to tissue destruction or fibrosis, respectively.[6,7] Control is achieved by external signals including cytokines (e.g. Interleukin (IL)-10, IL-27[8,9]) and hormones (e.g. glucocorticoids[10]) but also by MΦ-intrinsic mechanisms. For example, classically activated MΦ become unresponsive to secondary stimulation with lipopolysaccharide (LPS) due, at least in part, to the induction of negative feedback loops blocking or limiting activating signaling cascades.[11] The possibility that microRNAs may mediate such feedback-mechanisms, has recently attracted considerable interest.[11]

MicroRNAs (miRNA) are short (18-24nt), non-coding RNAs that influence the translation of specific genes by binding to the 3' untranslated region (3'UTR) of the target messenger RNAs (mRNAs). The interaction between a miRNA and mRNA generally results in destabilization of the mRNA and repression of translation.[12] In MΦ miRNAs have so far been mainly studied during classical activation where a number of

miRNAs have been found to be differentially regulated (reviewed in O'Neill et al[13]). miR-125b-5p is initially downregulated by LPS/TNF-induced Akt-signaling to allow efficient TNF-production,[14,15] but is induced during later stages where it acts to limit further TNF-production.[16] Similarly miR-146a-5p is upregulated upon LPS-stimulation and targets the MAPK-signaling pathway of TLRs, specifically IRAK1 and TRAF6.[17] Thus, these miRNAs are part of feedback-loops that prevent excessive MΦ activation and limit potentially harmful proinflammatory responses. Another M1-associated miRNA, miR-155, can suppress M2 activation by targeting the IL-13 receptor[18] suggesting that miRNAs are also involved in shaping the M1/M2 balance. Furthermore, miRNAs have been shown to control cellular proliferation,[19] which has potential relevance to M2 MΦ activation due to the recent discovery that MΦ-expansion can occur by IL-4-driven local proliferation rather than recruitment from the blood.[20] However, the miRNA-profile associated with alternative activation of MΦ has yet to be described. We therefore aimed to identify miRNAs differentially expressed in an *in vivo* model of alternative activation and dissect their functional roles. Microarray-analysis of MΦ elicited by exposure to the nematode *Brugia malayi*[5,21] identified miR-378-3p as one of the most robustly regulated miRNAs in this Th2 infection context, and *in vitro* experiments demonstrated that miR-378-3p was induced upon IL-4 stimulation. *In silico* analysis and miRNA manipulation studies identified potential miR-378-3p-targets in the PI3K/Akt-signaling cascade, downstream of the IL-4 receptor. The finding that Akt was a target of miR-378-3p led us to test the consequences of Akt inhibition revealing this signaling pathway as a critical component of IL-4 driven MΦ proliferation and alternative activation *in vivo*. Thus, it is

likely that miRNAs are a general mechanism for limiting MΦ activation in both alternative and classical activation settings.

Materials and Methods

Mice and Infection

Wild-type (WT, BALB/c or C57BL/6) and IL-4 Receptor-alpha deficient (IL-4Rα-/-) mice on a BALB/c background were bred in house. Mice were 6-10 weeks old at the start of each experiment and all work was performed in accordance with the UK Animals (Scientific Procedures) Act of 1986. Adult *B. malayi* parasites were isolated from the peritoneal cavity of infected Jirds purchased from TRS Laboratories or maintained in house. Infections were carried out as described previously.[21] A detailed description and additional information can be found in the supplementary material available online.

MΦ-isolation and purification

PEC were seeded at 5x10^6 cells per well to 6-well cell-culture plates (NUNC) in RPMI, 5% FCS, 2 mM L-glutamine, 0.25 U/mL penicillin and 100 mg/mL streptomycin. After 4 hours incubation at 37 °C / 5% CO_2 non-adherent cells were washed off and the adherent cells detached using a rubber-policeman. Detached cells were > 80% pure MΦ as assessed by flow-cytometry (FACS) analysis of their F4/80 and CD11b surface expression. In some experiments as indicated peritoneal MΦ were purified using FACS-sorting on a FACSAria cell sorter (BD Biosciences) according to their expression of surface molecules (F4/80+, SiglecF-, CD11b+, CD11c-, B220-, CD3-; all antibodies purchased from BioLegend or eBioscience) reaching purities of above 90%.

Cell-culture experiments

For *in vitro* experiments thioglycollate-elicited PEC were seeded to 24-well plates at 1x10^6 cells per well in complete RPMI. After 4 hours incubation, non-adherent cells were washed off and murine recombinant IL-4 (rIL-4, 20ng/mL, Peprotech), recombinant macrophage colony stimulating factor (rM-CSF, 20ng/ml, Peprotech), LPS (100ng/mL; *Escherichia coli* 0111:B4; Sigma-Aldrich) and recombinant Interferon-γ (rIFNγ, 20ng/mL, Peprotech) or medium alone were added and incubated for various periods of time as indicated in the text. For triciribine (1,5-dihydro-5-methyl-1-β-D-ribofuranosyl-1,2,5,6,8-pentaazaacenaphthylen-3-amine; Cayman Europe) treatment, cells were pretreated for 1 hour (see text for concentrations) prior to stimulation. Subsequently non-adherent cells were washed off and the remaining cells lysed in 700 μL Qiazol.

miRNA MicroArray

The miRCury miRNA probe set version 8.1 (Exiqon) was printed onto Codelink slides (GE Healthcare) in triplicate per array. Arrays were spot-checked using random hexamer-labelled RNAs. For experiments in this report, RNA (1 μg) was labelled using the Hy3 power labelling kit (Exiqon) and hybridization and washing were carried out following the manufacturer's instructions.

Array analysis was carried out using a comparative strategy in order to identify robustly regulated miRNAs. The background subtracted data were quantile normalized and the probes recognizing murine miRNA were selected to minimize the multiple testing problem. Medians were calculated for each miRNA per group (n = 4) and expression compared by t-test (WT v IL-4Rα-/- and WT v Thio). The regulated miRNA in each

comparison were then selected based on those with two or more significantly regulated probes and a log2 median intensity on the array greater than the 50th percentile. Our second analysis strategy used the limma suite[22] in bioconductor.[23] A linear model was fitted to each probe across all four groups and regulated miRNAs extracted by contrast. Similarly to our analysis of medians we selected miRNAs as regulated if two or more probes for the miRNA had significant uncorrected p-values and the median was greater than the 50th percentile. The lists from each analysis were then examined and overlapping miRNAs chosen for follow-up analysis. Microarray data have been deposited to NCBI's Gene Expression Omnibus and are accessible through GEO Series accession number GSE35047.

Dual-Luciferase Reporter Assay

Whole 3'UTRs of target genes (i.e. *Akt1*, *Grb2*) were cloned into the psiCHECK™-2 vector (Promega) immediately downstream of the *Renilla* luciferase gene. Mutations in the 3'UTR of *Akt1* or *Grb2* were generated using the QuikChange Lightning Multi Site-Directed Mutagenesis Kit (Stratagene) resulting in altered binding sites for miR-378-3p (AGUCCAG -> AGUGGAG). NIH-3T3 fibroblasts were cotransfected with 200 ng of the psiCHECK™-2 constructs and 2.5 pmol synthetic miR-378-3p precursor (hsa-miR-378 premiR™, Applied Biosystems) or scrambled miRNA control (premiR™ neg. control #1; Applied Biosystems) using Lipofectamine 2000 (Invitrogen). 48 hours post transfection relative luminescence was measured using the Dual-Luciferase® Reporter Assay System (Promega) on a LumiStar luminometer (BMG Labtechnologies) following the manufacturer's instructions. Resulting luminescence values were used to generate ratios

of *Renilla* to firefly luciferase activity and are depicted as fold change compared to a no-RNA transfected control for each construct.

Affymetrix messenger RNA array and data analysis

To determine genes potentially regulated by miR-378-3p NIH-3T3 cells were reverse transfected with a miR-378-3p mimic or inhibitor (25 nM) and compared to control-transfected (RISC-free-siRNA) cells. 300 ng of total RNA were converted to cDNA using the GeneChip WT cDNA Synthesis and Amplification Kit (Affymetrix) and hybridized to Affymetrix GeneChip ® Mouse Gene 1.0 ST Array according to the manufacturer's instructions. For the bioinformatic analysis, Partek Genomics Suite version 6.5 software (Partek Inc.) was used to assess the Genechip quality control and perform gene expression analysis utilizing Affymetrix metafiles. Data from nine chips met the quality control requirements thereby all were included. RMA method was used to normalize and summarize the intensity levels of all 28,853 probes.[24] Based on the (log 2 value) of negative control probes of each chip, the background fluorescence was calculated in StatPlus statistical tool pack software (AnalystSoft) and then used to statistically eliminate the microarray's background noise generating a list of 12665 probes. Partek's software computed the fold change and statistical significance (FDR adjusted *P* value) using one-way ANOVA test. Microarray data have been deposited to NCBI's Gene Expression Omnibus and are accessible through GEO Series accession number GSE34873.

In vivo IL-4 complex treatment

MΦ proliferation in vivo was stimulated by intraperitoneal injection of 5 μg rIL-4 complexed to 25 μg anti-IL-4 antibody (IL-4c; clone:11B11; molar ratio 2:1).[20] Where indicated mice were pretreated intraperitoneally with triciribine (1 mg/kg) 1 hour prior to injection of IL-4c. 21 hours post IL-4c injection mice received 100 μL of BrdU (10mg/mL, Sigma Aldrich) s.c. and peritoneal exudate cells (PEC) were harvested three hours later.

MΦ transfection experiments

RAW264.7 cells were stained with 5μM Vybrant®CFDA SE cell tracer kit (Invitrogen) followed by reverse transfection with a miR-378-3p mimic or inhibitor (25 nM) as described above and analysed for cellular expansion after 24 h and 48 h. Four hours prior to the end of the incubation 100 μL alamarBlue® were added to the culture. Cell proliferation was analysed by measuring alamarBlue® conversion in a FluoStar (BMG Labtechnologies) fluorescence plate reader and Vybrant®CFDA SE dilution by FACS-analysis. Data were pooled from three experiments and are presented as percent of control to account for inter-experimental changes in staining intensity.

Statistical analysis

Statistical analysis was performed using JMP statistical analysis software (JMP 8.0.1; SAS Institute Inc.). Differences between groups were determined by ANOVA followed by a Tukey-Kramer HSD multiple comparison-test. In some cases data was log-transformed to achieve normal distribution as determined by optical examination of

residuals, or where this was not possible a Kruskal-Wallis test was used. Differences were considered statistically significant for *P* values of less than 0.05.

Results

To identify miRNAs differentially regulated in alternatively activated MΦ *in vivo* we performed a miRNA array screen on peritoneal MΦ isolated from mice surgically implanted with the parasitic nematode *B. malayi*. As described previously, *B. malayi* implant results in a very strongly Th2-biased immune response and induces the accumulation of alternatively activated MΦ at the site of implantation.[5] For comparison, we used IL-4Rα-deficient (IL-4Rα$^{-/-}$) animals whose MΦ fail to express alternative activation markers in this model.[25] Additional wildtype (WT) mice underwent sham surgery and were injected with thioglycollate 3 days prior to necropsy in order to generate inflammatory MΦ not associated with helminth infection. A two-way comparison of WT nematode elicited MΦ (NeMΦ) with thioglycollate-elicited MΦ (Thio-MΦ) or IL-4Rα$^{-/-}$ NeMΦ allowed us to identify infection-dependent and IL-4Rα-dependent miRNAs respectively. Three weeks post implant MΦ were isolated from the peritoneal cavity by adherence to cell-culture plates and total RNA extracted as described in materials and methods. The expression levels of 648 unique human and mouse miRNAs in their mature form were determined using the Exiqon miRCury 8.1 array platform. Bioinformatic analysis (see Materials and Methods for details) revealed differential expression of 19 miRNAs in WT-NeMΦ compared to either Thio-MΦ or IL-4Rα$^{-/-}$ NeMΦ (Suppl.table S2).

We then chose to validate expression levels of the 10 most differentially regulated miRNAs (i.e. highest fold change) identified in the array. A proportion of the originally isolated RNA was subjected to quantitative RT-PCR (qRT-PCR), with further analysis in two subsequent experiments using FACS-sorted MΦ (>90% F4/80+CD11b+). These

experiments confirmed significant differential expression of 9 of these 10 miRNAs, but also revealed that only four of these were differentially regulated in both comparisons (WT NeMΦ versus WT Thio-MΦ and versus IL-4Rα$^{-/-}$ NeMΦ) and therefore specific for alternatively activated MΦ (Table 1 & Figure 1A). miR-125b-5p, miR-199b-5p and miR-378-3p, were found to be significantly up-regulated *in vivo* whereas miR-146a-5p showed a tendency towards an IL-4Rα-dependent downmodulation (Figure 1A). This tendency in miR-146a-5p expression was statistically significant (*P*=.0022) when all three experiments were combined. To confirm the activation state of the isolated MΦ, expression of the alternative activation marker chitinase 3-like 3 (*Chi3l3*/Ym1) was measured and, as expected, found to be exclusively upregulated in WT NeMΦ but not in IL-4Rα$^{-/-}$ MΦ (Figure 1B).

It was possible that the changes we observed were the result of secondary (IL-4Rα-dependent) events occurring *in vivo* and not due to direct MΦ activation via IL-4/13. Thus, we tested the expression of miR125b-5p, miR-146a-5p, miR-199b-5p and miR-378-3p in Thio-MΦ stimulated *in vitro* with rIL-4 or LPS and rIFNγ (Figure 1C). Quantitative RT-PCR revealed significant upregulation of miR-125b-5p and miR-378-3p upon IL-4 treatment but not upon LPS/IFNγ-stimulation confirming the association of these miRNAs with the alternative activation phenotype. In contrast miR-199b-5p was not altered either by IL-4 or LPS/IFNγ treatment indicating that the observed upregulation *in vivo* is not due to direct effects of IL-4R-signaling on MΦ. miR-146a-5p has previously been found to be highly upregulated in classically activated MΦ[17] and was consequently specifically induced upon LPS/IFNγ stimulation but no change in expression could be detected upon IL-4-stimulation *in vitro* at this time point (Figure 1C).

Successful and specific induction of alternative activation under these conditions was confirmed by *Chi3l3*-expression (Figure 1D).

miR-125b-expression in MΦ has previously been demonstrated to be modulated by factors other than IL-4.[15,16] We selected miR-378-3p for further investigation into its potential to regulate alternative activation of MΦ because it appeared to be the most specific for IL-4Rα-mediated signals. Further, miR-378-3p was of particular interest because it is encoded in an intronic region of the peroxisome proliferative activated receptor, gamma, coactivator 1 beta gene (*Ppargc1b)*,[26] which has previously been shown to be associated with the alternative activation phenotype.[27]

To evaluate whether upregulation of miR-378-3p was a prerequisite for alternative MΦ activation or a consequence thereof, we performed *in vitro* timecourse experiments of IL-4 stimulation (Figure 2) in which Thio-MΦ were incubated with murine rIL-4 for 1, 4, 16, 28 and 45 hours. Cells were subsequently analysed for mRNA and miRNA expression using qRT-PCR. Significantly increased levels of *Chi3l3* expression were detectable as early as 4 hours after treatment of MΦ with IL-4 and continued to rise until the end of the experiment. In contrast miR-378-3p was not significantly upregulated until 16 hours after the addition of IL-4 but remained elevated thereafter. Notably, classical activation of MΦ using LPS/IFNγ did not result in the upregulation of *Chi3l3* or miR-378-3p at any timepoint, but potently induced expression of inducible nitric oxide synthase 2 (*Nos2*) and miR-146a-5p as described previously.[17,28] Interestingly, in line with our *in vivo* data (Figure 1A), miR-146a-5p was significantly reduced following IL-4-stimulation at very late timepoints (45 hours) but not at 24 hours. This might explain why we were unable to

detect a direct effect of IL-4 on miR-146a-5p expression in the previous *in vitro* experiments measured at 16 hours post treatment (Figure 1C).

In order to examine cellular genes that respond to changes in miR-378-3p expression, we used a murine fibroblast cell line that expresses miR-378-3p and supports miRNA over-expression and inhibition analysis, as described.[29] NIH-3T3-fibroblasts were transfected with either miR-378-3p-mimics or –inhibitors and resulting changes in gene-expression analysed utilizing an Affymetrix-mRNA-array. We were able to identify 491 significantly differentially expressed genes (FDR $P < .05$) with more than 1.4 fold change in either of the two conditions as compared to a negative-control (RISC-free). Pathway analysis of these differentially expressed genes using DAVID Bioinformatics Resources for gene annotation and KEGG pathway analysis (http://david.abcc.ncifcrf.gov/tools.jsp) revealed the Jak-STAT signaling pathway as significantly targeted (EASE-score $P < .05$). More specifically in conjunction with the online prediction software Targetscan (TargetScanMouse; Release 5.1:April2009; www.targetscan.org) several potential target-genes within the IL-4Rα/PI3K/Akt-signaling cascade could be identified. Figure 3A illustrates the components of the IL-4Rα pathway that were predicted by target scan (yellow) and differentially expressed in transfected fibroblasts (red). In particular Akt-1 was identified in both analyses. This suggested the possibility that IL-4 induction of miR-378-3p results in a negative feedback on the IL-4 signaling pathway. Because receptor 'tolerance' has not previously been described for this pathway, we tested whether IL-4 does induce a negative feedback-mechanism by measuring STAT-6-phosphorylation in Thio-MΦ following secondary IL-4 stimulation. As outlined in Figure 3B, MΦ that had

previously been exposed to IL-4 showed reduced and delayed STAT-6 phosphorylation in response to secondary IL-4 stimulation.

To obtain direct evidence that miR-378-3p targets the PI3k/Akt1-pathway we generated Luciferase-constructs containing the 3'UTR of thymoma viral proto-oncogene 1 (*Akt1*) or a mutated version thereof, where two nucleotides within both seed-region-binding sites for miR-378-3p were altered (Suppl.Figure 1A). As shown in Figure 3C, co-transfecting NIH-3T3-fibroblasts with a mimic of miR-378-3p significantly inhibited Luciferase expression as compared to cells transfected with the Luciferase-construct alone, or co-transfected with a negative control RNA. Importantly these effects were lost when both miR-378-3p-binding sites within the *Akt1* - 3'UTR were mutated. Furthermore transfection of RAW264.7 cells led to a marked decrease in Akt-1 protein levels as assessed by Western Blot analysis ($P < .01$ in every comparison) (Figure 3D&E). Similar results were obtained for growth factor receptor bound protein 2 (*Grb2*), ($P < .05$) (Suppl.Figure 1B-D). Interestingly use of a miR-378-3p inhibitor increased protein-expression of Akt-1 in some experiments, but this was not significant when the data of several experiments was combined (Figure 2D&E).

The identification of Akt as a target of miR-378-3p led us to assess the potential influence of Akt-inhibition on MΦ alternative activation using a specific Akt-inhibitor (triciribine[30]) (Figure 4). Preincubation of Thio-MΦ with triciribine severely disrupted their ability to fully alternatively activate in a dose-dependent manner as shown for the expression of *Chi3l3*, resistin like alpha (*Retnla*/Relm-α) and arginase 1 (*Arg1*) (Figure 4). Of note, Akt-inhibition differentially affected expression of these markers with complete abrogation of IL-4 driven *Retnla*- but only partial inhibition of *Chi3l3*- and

Arg1-induction. In contrast other marker genes of alternative MΦ activation (e.g. *Cd36*, *Pparg*, *Ppargc1b*) were not negatively influenced by the inhibition of Akt. Thus limiting Akt-signaling does not completely block IL-4 mediated alternative activation, but changes the associated gene expression profile, perhaps to generate cells better suited to chronic type-2 inflammatory settings.

We recently demonstrated that proliferation of the local MΦ population is an integral part of Th2 mediated inflammation with no requirement for blood monocyte recruitment.[20] The expansion in cell numbers following surgical implantation of *B. malayi* nematodes occurs as an early burst of rapid cellular proliferation which then subsides.[20(fig. S4)] Of note, RNA isolated from these MΦ revealed a delayed increase in miR-378-3p expression peaking when MΦ proliferation subsided and Akt1 gene-expression declined (Figure 5). Critically, injection of active IL-4 alone can drive this proliferative programme *in vivo*. Because both miRNAs and the PI3K/Akt-pathway are inherently associated with cellular growth and proliferation, we speculated that IL-4 driven MΦ proliferation is mediated via Akt signaling, with miR-378-3p and possibly other miRNAs acting as negative regulators. We thus chose to test the role of Akt-signaling during IL-4 mediated MΦ-proliferation. For this mice received a single dose of triciribine or vehicle control i.p. one hour prior to injection of IL-4 complexed with anti IL-4 antibody (IL-4c) which allows sustained delivery of active cytokine.[20] After 21 hours mice were injected with BrdU to label cells in S-phase and three hours later peritoneal exudate cells analysed for expression of proliferation- and alternative activation markers by flow cytometry. Pretreatment with triciribine completely abrogated IL-4c induced MΦ proliferation as measured by the incorporation of BrdU or expression of Ki67 (Figure 6A).

Simultaneously protein levels of the alternative activation marker Relm-α was only partially reduced and YM-1 expression did not seem affected at all. These data indicate that similar to the effects observed *in vitro*, IL-4 induced Akt-signaling is responsible for only specific features of alternative MΦ activation, but is essential for IL-4 driven proliferation.

Furthermore to establish a role for miR-378-3p in the regulation of MΦ proliferation we transfected RAW264.7 cells with a miR-378-3p mimic or -inhibitor and analysed the resulting changes in cellular expansion. Conversion of alamarBlue® and loss of Vybrant®CFDA SE staining were used to monitor cell expansion and cell division, respectively. Over a 24 hr period, cells transfected with the miR-378-3p mimic displayed a significantly reduced increase in the conversion of alamarBlue® (Figure 6B) and loss of Vybrant®CFDA SE staining (Figure 6C) demonstrating that miR378-3p negatively regulated cell proliferation. Transfection with the miR-378-3p inhibitor had no effect on cellular expansion indicating that only enhanced miR-378-3p expression as found after IL-4 stimulation regulates proliferation. What is more, gene-expression analyses of RAW264.7 cells transfected with miR-378-3p showed significant reduction in expression of *Akt-1* and *Grb2*, as well as the putative target *Pik3cb* (Figure 3A) and the proliferation marker *Mki67* (Figure 6D). Taken together these results are consistent with a negative regulation of MΦ proliferation by miR-378-3p through modulation of the PI3K/Akt-signaling pathway.

IL-4 impacts on the activation state of many cell types and the PI3K/Akt pathway regulates cellular expansion in various biological settings. Thus, to determine whether induction of miR-378-3p and therefore potential regulation of PI3K/Akt signaling, was a

general characteristic of either MΦ proliferation or IL-4 signaling in other cell-types, we analysed miR-378-3p expression in MΦ during IL-4 independent, M-CSF driven proliferation and in B- and T-cells following IL-4c stimulation *in vivo*. As expected, Thio-PMΦ treated with rM-CSF *in vitro* stimulated MΦ proliferation as confirmed by increased gene expression of *Mki67* (Figure 7A). However, at no timepoint post stimulation could induction of miR-378-3p or its parent gene (*Ppargc1b*) be detected. Similarly enhanced expression of miR-378-3p and *Ppargc1b* following IL-4c injection *in vivo* was found in peritoneal MΦ (F4/80+CD11b+) but not in B-cells (CD19+F4/80-), CD4+ (CD4+CD11b-) or CD8+ lymphocytes (CD8+CD11b-) isolated from the same animal (Figure 7B). Of note, IL-4c has previously been shown to also induce proliferation of CD8+ lymphocytes[31] as confirmed in our data by increased expression of cyclin A2 (*Ccna2*). The failure to induce miR-378-3p in these cells as well as in M-CSF stimulated macrophages indicates, that miR-378-3p is not a general feature of cellular proliferation whether IL-4 dependent or independent. Furthermore, the lack of induction of miR-378-3p in other cells stimulated with IL-4c shows, that although IL-4 signaling has widespread effects on various cell-types, the mechanisms controlling these effects are governed by different regulatory mechanisms. Induction of miR-378-3p therefore appears to be a very specific feature of alternative MΦ activation.

Discussion

MΦ isolated from mice infected with the human filarial parasite *B.malayi* become alternatively activated due to exposure to Th2 cells.[21] In this *in vivo* setting, we have identified changes in MΦ expression of miR-125b-5p, miR-199b-5p, miR-378-3p and miR-146a-5p associated with IL-4Rα-driven alternative activation. *In vitro* confirmation revealed that miR-125b-5p, miR-378-3p and miR-146a-5p were directly regulated by IL-4 whereas miR-199b-5p was not, suggesting miR-199b-5p is induced *in vivo* by other factors and/or that IL-4 is not sufficient. Interestingly another miRNA, miR-223-3p, has recently been described to be associated with the alternative activation phenotype.[32] Indeed, miR-223-3p was significantly enhanced in WT NeMΦ vs. IL-4Rα-/- NeMΦ in our array but was not among the most highly differentially expressed microRNAs in this *in vivo* setting and thus not pursued in this study.

Both miR-125b-5p and miR-146a-5p have already been associated with classical MΦ activation. miR-125b-5p expression is initially reduced following LPS-stimulation allowing efficient production of its target, the proinflammatory cytokine TNF-α[15] but miR-125b-5p is then upregulated during LPS-tolerance to prevent further/excessive TNF-production.[16] Thus, miR-125b-5p upregulation in alternatively activated MΦ may represent a failsafe-switch preventing concomitant production of proinflammatory mediators like TNF-α. miR-146a-5p on the other hand is normally induced following classical activation of monocytes and is presumed to act in a feedback loop blocking further TLR- and cytokine-signaling.[17,33] Down-modulation of this miRNA in IL-4 stimulated MΦ could enhance TLR-signaling and thus seems counterintuitive. However,

reduced levels of miR-146a-5p did not occur until very late following IL-4 stimulation (Figure 3) and longterm pre-incubation of MΦ with IL-4 has previously been shown to potentiate production of proinflammatory cytokines following secondary stimulation with LPS.[34] Thus, whereas upregulation of miR-125b-5p might help prevent concomitant production of inflammatory mediators, miR-146a-5p-downmodulation may simultaneously sensitise MΦ for potential bacterial pathogens and allow MΦ to quickly adapt their activation phenotype to newly arising challenges. Further experiments are needed to determine the exact role of these two miRNAs in shaping MΦ activation.

Here we focus on the new finding that upregulation of miR-378-3p is part of the alternative MΦ activation programme. This is consistent with a report that miR-378-3p is upregulated in a model of allergic airway inflammation.[35] Although the authors did not perform cell-type specific analyses, the inflammatory response in these models is characterised by the accumulation of MΦ exhibiting an alternative activation phenotype.[36] As noted above, miR-378-3p is encoded in an intronic region of *Ppargc1b*,[26] a protein associated with alternative activation.[27] Thus coexpression of miR-378-3p may have evolved to complement the role of the protein-encoding gene.[37] *Ppargc1b* is expressed by 4 hours following IL-4 stimulation and this would suggest that *Ppargc1b* and the primary transcript of mir-378-3p, are primary targets of IL-4 induced gene transcription. However, the mature form of miR-378-3p is delayed with respect to its parent gene and other alternative activation markers and thus secondary factors may be needed to regulate its processing.

We identified several miR-378-3p targets within the IL-4R-signaling cascade and more specifically within the PI3K/Akt-signaling pathway. Previous work by MacKinnon et al[38]

showed that signaling via PI3K is important for full alternative activation of MΦ and we have extended these findings by using the Akt-specific inhibitor triciribine confirming Akt as an important downstream target of PI3K during IL-4 induced alternative activation. Interestingly Varin et al[39] showed that pre-treatment of MΦ with IL-4 prevented subsequent Akt-signaling induced by *Neisseria meningitidis* suggesting the induction of a feedback inhibitory mechanism by IL-4. Importantly these effects were not observed until approximately 12 hours post IL-4 stimulation, a timepoint which roughly coincides with the induction of miR-378-3p in our experiments. In addition miR-378-3p has been predicted to target the progesterone-receptor[40] and progesterone has been shown to be an important enhancement factor for alternative activation in wound healing.[41] Taken together these findings strongly suggest a role for miR-378-3p as feedback inhibitor of alternative activation. In this context PI3K/Akt signaling has been shown to enhance anti-inflammatory cytokine production during classical MΦ activation and simultaneously reduce production of pro-inflammatory cytokines.[42] Thus, induction of miR-378-3p and limitation of Akt-signaling in alternatively activated MΦ could, similar to our findings with miR-146a-3p, indicate a sensitisation for potential concomitant bacterial infections.

PI3K/Akt is a central signaling pathway important for cellular growth and survival, triggered by various growth factors and insulin, but also by cytokines and TLR-stimulation.[43] Although tissue MΦ have been typically regarded as non-dividing, recent data shows that resident MΦ numbers can be maintained by proliferation.[20,44,45] We further demonstrated that tissue MΦ can undergo rapid and extensive proliferation *in vivo* in response to IL-4 as a mechanism of Th2-driven inflammation that can replace

monocyte recruitment.[20] Using triciribine we show here that, similar to the findings *in vitro*, intact PI3K/Akt-signaling enhances alternative activation of MΦ *in vivo* but moreover is absolutely essential for IL-4 induced MΦ proliferation. In a related context miR-378-3p has been shown to be upregulated during differentiation of proliferating myoblasts to non-proliferating myotubes and consequently severely downmodulated in cardiotoxin induced muscle-regeneration.[46] Similarly in a model of surgically induced liver injury downmodulation of miR-378-3p has been proposed to allow efficient hepatocyte proliferation by derepressing pro-proliferative molecules like ornithine decarboxylase.[47] A human ortholog of miR-378-3p with identical mature sequence, miR-422a, has, in concert with other miRNAs, been proposed to block proliferation of tumor cells by targeting the MAPK pathway.[48] Taken together with our observation that miR-378-3p negatively regulated RAW264.7 cell-expansion, these results suggest that miR-378-3p is centrally involved in the control of proliferation. Indeed some of the main pathways identified as potential targets for miR-378-3p in our bioinformatic pathway analysis of transfected fibroblasts, in addition to the Jak/Stat-signaling pathway, included cell cycle, p53- and MAPK signaling pathways, which merit further validation. Importantly our data indicates, that despite miR-378-3p having the potential to control proliferation in various cell-types and under multiple settings, its induction under normal conditions seems restricted to IL-4 activated MΦ. Most likely this reflects the fact that miR-378-3p will target other, as yet undefined target genes besides *Akt1* and thus have a much broader effect on the cellular phenotype, than discussed here.

We have been unable to demonstrate significant MΦ proliferation with IL-4 *in vitro* suggesting that additional signals to the cell, either through cell-cell contacts, or as yet

undefined soluble mediators are required. Additionally, miRNAs do not typically induce complete knockdown of their targets,[12] and miRNAs often act in families targeting a whole metabolic or signaling pathway rather than individual members of these pathways leading to a general suppression of whole metabolic or activation programmes.[49] Further, *in vivo* MΦ transfection with miRNAs is challenging. For these reasons it remains to be directly demonstrated whether miR-378-3p, possibly in combination with other miRNAs regulates MΦ proliferation via Akt inhibition *in vivo*. We have circumstantial evidence showing that peak proliferation of MΦ following *B.malayi* implant precedes miR-378-3p induction and this is paralleled by a concomitant downregulation in *Akt1*-expression (Fig. 5). Similarly transfection of RAW264.7 cells with miR-378-3p reduced expression of PI3K/Akt-pathway molecules and negatively impacted on cellular expansion.

Beyond the putative link between miR-378-3p and IL-4 driven macrophage proliferation, this study has generated the novel and important finding that miR-378-3p is an IL-4-dependent miRNA upregulated in MΦ, both *in vitro* and *in vivo* which targets the Akt-signaling pathway. Importantly, this finding has led to the independent observation that the local MΦ proliferation that occurs during Th2 mediated inflammation relies on Akt. This has important therapeutic implications as PI3K/Akt inhibitors are already being developed to target proliferation during cancer[50,51] and thus might have off target effects on MΦ. Additionally, efforts to target this pathway may generate important therapeutics to control MΦ proliferation, which is believed to exacerbate diseases such as glomerulonephritis and atherosclerosis.[52,53]

Acknowledgements:

We thank Yvonne Harcus for excellent technical assistance, Martin Waterfall for performing outstanding FACS-sorting and Frank Brombacher for providing the IL-4Rα$^{-/-}$ mice.

This work was funded by the MRC UK (MRC-UK G0600818) and the Wellcome Trust (Centre for Immunity, Infection and Evolution; 082611/Z/07/Z). The funders had no role in study design, data collection and analysis, decision to publish or preparation of the manuscript.

Authorship:

Contribution: D.R. designed and performed research, analysed and interpreted data and wrote the manuscript. S.J.J. performed research, analysed and interpreted data and contributed vital new analytical tools. N.N.L. performed research, analysed and interpreted data. I.J.G. analysed and interpreted data. T.E.S. contributed vital new tools. S.D. performed research. A.H.B. and J.E.A. contributed to data interpretation, manuscript preparation and project supervision.

Conflict-of-interest disclosure: The authors declare no competing financial interests.

Correspondence: Judith E. Allen, The University of Edinburgh, Institute of Immunology and Infection Research, Ashworth Laboratories, West Mains Rd, EH9 3JT Edinburgh, UK; e-mail: j.allen@ed.ac.uk.

References:

1. Gordon S. Alternative activation of macrophages. *Nat Rev Immunol*. 2003;3(1):23-35.
2. Biswas SK, Mantovani A. Macrophage plasticity and interaction with lymphocyte subsets: cancer as a paradigm. *Nature Immunology*. 2010;11(10):889-896.
3. Díaz A, Allen JE. Mapping immune response profiles: The emerging scenario from helminth immunology. *Eur J Immunol*. 2007;37(12):3319-3326.
4. Gordon S, Martinez FO. Alternative activation of macrophages: mechanism and functions. *Immunity*. 2010;32(5):593-604.
5. Loke Pn, Nair MG, Parkinson J, Guiliano D, Blaxter M, Allen JE. IL-4 dependent alternatively-activated macrophages have a distinctive in vivo gene expression phenotype. *BMC Immunol*. 2002;3:7.
6. Martinez FO, Sica A, Mantovani A, Locati M. Macrophage activation and polarization. *Front Biosci*. 2008;13:453-461.
7. Murray PJ, Wynn TA. Obstacles and opportunities for understanding macrophage polarization. *J Leukoc Biol*. 2011;89(4):557-563.
8. Hölscher C, Hölscher A, Rückerl D, et al. The IL-27 receptor chain WSX-1 differentially regulates antibacterial immunity and survival during experimental tuberculosis. *J Immunol*. 2005;174(6):3534-3544.
9. Lang R, Patel D, Morris JJ, Rutschman RL, Murray PJ. Shaping gene expression in activated and resting primary macrophages by IL-10. *J Immunol*. 2002;169(5):2253-2263.
10. Rhen T, Cidlowski JA. Antiinflammatory action of glucocorticoids--new mechanisms for old drugs. *N Engl J Med*. 2005;353(16):1711-1723.
11. Ivashkiv LB. Inflammatory signaling in macrophages: Transitions from acute to tolerant and alternative activation states. *Eur J Immunol*. 2011;41(9):2477-2481.
12. Guo H, Ingolia NT, Weissman JS, Bartel DP. Mammalian microRNAs predominantly act to decrease target mRNA levels. *Nature*. 2010;466(7308):835-840.
13. O'neill LA, Sheedy FJ, McCoy CE. MicroRNAs: the fine-tuners of Toll-like receptor signalling. *Nat Rev Immunol*. 2011;11(3):163-175.
14. Androulidaki A, Iliopoulos D, Arranz A, et al. The kinase Akt1 controls macrophage response to lipopolysaccharide by regulating microRNAs. *Immunity*. 2009;31(2):220-231.
15. Tili E, Michaille J-J, Cimino A, et al. Modulation of miR-155 and miR-125b levels following lipopolysaccharide/TNF-alpha stimulation and their possible roles in regulating the response to endotoxin shock. *J Immunol*. 2007;179(8):5082-5089.
16. El Gazzar M, McCall CE. MicroRNAs distinguish translational from transcriptional silencing during endotoxin tolerance. *J Biol Chem*. 2010;285(27):20940-20951.
17. Taganov KD, Boldin MP, Chang K-J, Baltimore D. NF-kappaB-dependent induction of microRNA miR-146, an inhibitor targeted to signaling proteins of innate immune responses. *Proc Natl Acad Sci USA*. 2006;103(33):12481-12486.

18. Martinez-Nunez RT, Louafi F, Sanchez-Elsner T. The interleukin 13 (IL-13) pathway in human macrophages is modulated by microrna-155 via direct targeting of interleukin 13 receptor alpha1 (IL13R{alpha}1). *J Biol Chem*. 2010;286(3):1786-1794.
19. Palma CA, Tonna EJ, Ma DF, Lutherborrow MA. MicroRNA control of myelopoiesis and the differentiation block in acute myeloid leukaemia. *J Cell Mol Med*. 2012;16(5):978-987.
20. Jenkins SJ, Ruckerl D, Cook PC, et al. Local Macrophage Proliferation, Rather than Recruitment from the Blood, Is a Signature of TH2 Inflammation. *Science*. 2011;332(6035):1284-1288.
21. Loke Pn, Gallagher I, Nair MG, et al. Alternative activation is an innate response to injury that requires CD4+ T cells to be sustained during chronic infection. *J Immunol*. 2007;179(6):3926-3936.
22. Smyth GK. Limma: linear models for microarray data. In: Gentleman R, Carey V, Huber W, Irizarry R, Dudoit S, eds. Bioinformatics and Computational Biology Solutions using R and Bioconductor. New York: Springer; 2005:397-420.
23. Gentleman RC, Carey VJ, Bates DM, et al. Bioconductor: open software development for computational biology and bioinformatics. *Genome Biol*. 2004;5(10):R80.
24. Bolstad BM, Irizarry RA, Astrand M, Speed TP. A comparison of normalization methods for high density oligonucleotide array data based on variance and bias. *Bioinformatics*. 2003;19(2):185-193.
25. Whyte CS, Bishop ET, Ruckerl D, et al. Suppressor of cytokine signaling (SOCS)1 is a key determinant of differential macrophage activation and function. *J Leukoc Biol*. 2011;90(5):845-854.
26. Eichner LJ, Perry MC, Dufour CR, et al. miR-378(*) mediates metabolic shift in breast cancer cells via the PGC-1beta/ERRgamma transcriptional pathway. *Cell Metab*. 2010;12(4):352-361.
27. Vats D, Mukundan L, Odegaard JI, et al. Oxidative metabolism and PGC-1beta attenuate macrophage-mediated inflammation. *Cell Metab*. 2006;4(1):13-24.
28. Mosser DM. The many faces of macrophage activation. *J Leukoc Biol*. 2003;73(2):209-212.
29. Santhakumar D, Forster T, Laqtom NN, et al. Combined agonist-antagonist genome-wide functional screening identifies broadly active antiviral microRNAs. *Proceedings of the National Academy of Sciences*. 2010;107(31):13830-13835.
30. Sun J, Ramnath RD, Tamizhselvi R, Bhatia M. Role of protein kinase C and phosphoinositide 3-kinase-Akt in substance P-induced proinflammatory pathways in mouse macrophages. *The FASEB Journal*. 2009;23(4):997-1010.
31. Boyman O, Kovar M, Rubinstein MP, Surh CD, Sprent J. Selective stimulation of T cell subsets with antibody-cytokine immune complexes. *Science*. 2006;311(5769):1924-1927.
32. Zhuang G, Meng C, Guo X, et al. A Novel Regulator of Macrophage Activation: miR-223 in Obesity Associated Adipose Tissue Inflammation. *Circulation*. 2012.
33. Jurkin J, Schichl YM, Koeffel R, et al. miR-146a is differentially expressed by myeloid dendritic cell subsets and desensitizes cells to TLR2-dependent activation. *J Immunol*. 2010;184(9):4955-4965.

34. D'Andrea A, Ma X, Aste-Amezaga M, Paganin C, Trinchieri G. Stimulatory and inhibitory effects of interleukin (IL)-4 and IL-13 on the production of cytokines by human peripheral blood mononuclear cells: priming for IL-12 and tumor necrosis factor alpha production. *J Exp Med*. 1995;181(2):537-546.
35. Lu TX, Munitz A, Rothenberg ME. MicroRNA-21 is up-regulated in allergic airway inflammation and regulates IL-12p35 expression. *J Immunol*. 2009;182(8):4994-5002.
36. Melgert BN, Oriss TB, Qi Z, et al. Macrophages: regulators of sex differences in asthma? *Am J Respir Cell Mol Biol*. 2010;42(5):595-603.
37. van Rooij E, Quiat D, Johnson BA, et al. A family of microRNAs encoded by myosin genes governs myosin expression and muscle performance. *Dev Cell*. 2009;17(5):662-673.
38. Mackinnon A, Farnworth S, Hodkinson P, et al. Regulation of Alternative Macrophage Activation by Galectin-3. *J Immunol*. 2008;180(4):2650-2658.
39. Varin A, Mukhopadhyay S, Herbein G, Gordon S. Alternative activation of macrophages by IL-4 impairs phagocytosis of pathogens but potentiates microbial-induced signalling and cytokine secretion. *Blood*. 2010;115(2):353-362.
40. Zhou J, Song T, Gong S, Zhong M, Su G. microRNA regulation of the expression of the estrogen receptor in endometrial cancer. *Mol Med Rep*. 2010;3(3):387-392.
41. Routley CE, Ashcroft GS. Effect of estrogen and progesterone on macrophage activation during wound healing. *Wound repair and regeneration : official publication of the Wound Healing Society [and] the European Tissue Repair Society*. 2009;17(1):42-50.
42. Martin M, Rehani K, Jope RS, Michalek SM. Toll-like receptor-mediated cytokine production is differentially regulated by glycogen synthase kinase 3. *Nat Immunol*. 2005;6(8):777-784.
43. Weichhart T, Saemann MD. The PI3K/Akt/mTOR pathway in innate immune cells: emerging therapeutic applications. *Ann Rheum Dis*. 2008;67 Suppl 3:iii70-74.
44. Chorro L, Sarde A, Li M, et al. Langerhans cell (LC) proliferation mediates neonatal development, homeostasis, and inflammation-associated expansion of the epidermal LC network. *Journal of Experimental Medicine*. 2009;206(13):3089-3100.
45. Davies LC, Rosas M, Smith PJ, Fraser DJ, Jones SA, Taylor PR. A quantifiable proliferative burst of tissue macrophages restores homeostatic macrophage populations after acute inflammation. *Eur J Immunol*. 2011;41(8):2155-2164.
46. Gagan J, Dey BK, Layer R, Yan Z, Dutta A. MICRORNA-378 targets the myogenic repressor myor during myoblast differentiation. *J Biol Chem*. 2011;286:19431-19438.
47. Song G, Sharma AD, Roll GR, et al. MicroRNAs control hepatocyte proliferation during liver regeneration. *Hepatology*. 2010;51(5):1735-1743.
48. Gougelet A, Pissaloux D, Besse A, et al. Micro-RNA profiles in osteosarcoma as a predictive tool for ifosfamide response. *Int J Cancer*. 2011;129(3):680-690.
49. Xiao C, Rajewsky K. MicroRNA control in the immune system: basic principles. *Cell*. 2009;136(1):26-36.

50. Cheng JQ, Lindsley CW, Cheng GZ, Yang H, Nicosia SV. The Akt/PKB pathway: molecular target for cancer drug discovery. *Oncogene*. 2005;24(50):7482-7492.
51. Sarker D, Reid AHM, Yap TA, de Bono JS. Targeting the PI3K/AKT pathway for the treatment of prostate cancer. *Clin Cancer Res*. 2009;15(15):4799-4805.
52. Isbel NM, Nikolic-Paterson DJ, Hill PA, Dowling J, Atkins RC. Local macrophage proliferation correlates with increased renal M-CSF expression in human glomerulonephritis. *Nephrol Dial Transplant*. 2001;16(8):1638-1647.
53. Kuo CL, Murphy AJ, Sayers S, et al. Cdkn2a is an atherosclerosis modifier locus that regulates monocyte/macrophage proliferation. *Arterioscler Thromb Vasc Biol*. 2011;31(11):2483-2492.

Table 1: Log2 fold change of significantly differentially expressed microRNAs as assessed by microRNA-array or qRT-PCR. -: not significant.

microRNA-ID	BALB/c NeMΦ vs. BALB/c ThioMΦ		BALB/c NeMΦ vs. IL-4Rα$^{-/-}$ NeMΦ	
	Array	qRT-PCR	Array	qRT-PCR
miR-18a-5p	-1.31	- 1.01	-	-
miR-125b-5p	-	2.11	1.91	4.90
miR-146a-5p	-1.46	-1.47	-	-1.47
miR-150-5p	-	-	-1.97	- 2.15
miR-199b-5p	-	3.49	2.04	4.59
miR-221-3p	-1.53	- 2.11	-	-
miR-222-3p	-1.27	- 2.11	-	-
miR-342-3p	-1.51	- 1.81	-	-
miR-378-3p	2.10	2.42	2.28	2.14
miR-689	-	-	-2.56	-

Figure Legends:

Figure 1: Validation of differential expression of miRNAs in AAMΦ *in vivo* and *in vitro*.

(A) Peritoneal MΦ were isolated from thioglycollate-injected (Thio) BALB/c mice or from *B. malayi* infected BALB/c (WT) or IL-4Rα$^{-/-}$ (-/-) mice and expression of the indicated miRNAs assessed by qRT-PCR. Each data point shown reflects data from individual mice.

(B) *Chi3l3* expression in the cells isolated in A.

(C) Thioglycollate-elicited, adherence-purified MΦ were incubated with rIL-4 (IL-4), LPS/IFNγ (L/I) or without stimulus (-) for 16 hours and analysed as under A.

(D) *Chi3l3* expression in the cells isolated in C.

One of three separate experiments shown. * $P < .05$; ** $P < .01$; *** $P < .001$; n.s.: not significant

Figure 2: Kinetics of miR-378-3p-induction during *in vitro* alternative activation.

Thioglycollate-elicited, adherence-purified MΦ were incubated with rIL-4 (black squares), LPS and rIFNγ (grey triangles) or with medium alone (open rectangles) for the indicated time and analysed for mi-RNA and mRNA-expression. Statistics indicate differences between rIL-4-treated samples and media-controls. ** $P <$

.01; *** *P*< .001. Each data point represents mean and SEM of three individual animals. One of two separate experiments shown.

Figure 3: miR-378-3p targets the IL-4R/PI3K/Akt-signaling pathway.

(A) Schematic depiction of the IL-4R-signaling cascade depicting putative targets for miR-378-3p. Yellow: predicted by Targetscan; red: differentially expressed genes in pre- & anti-miR-378-3p transfected fibroblasts.

(B) Analysis of rIL-4 elicited STAT-6 phosphorylation by intracellular FACS-staining. Histogram of STAT-6(pY641) expression in Thio-MΦ pre-incubated with rIL-4 (orange line) or medium (red line) for 24 hours prior to restimulation with rIL-4 (open histograms) or medium (grey filled histograms) for 5 min. Timeline of pSTAT-6(pY641) expression in rIL-4 (orange squares) or medium (red circles) pretreated, rIL-4 stimulated (colored symbols) or unstimulated (grey symbols) cells. Data shows median fluorescence intensity of six individual animals +/-SEM. For unstimulated controls cells were pooled from several animals. Asterisks indicate statistical differences between rIL-4 pre-incubated and freshly stimulated MΦ. *** *P*< .001; ** *P*< .01.

(C) Luciferase-assay using the 3'UTR of wildtype Akt-1 (Akt-1) or constructs with mutated seed-region binding sites for both predicted miR-378-3p binding sites (mut) or without insert (empty). Data indicates cotransfection with a miR-378-3p mimic (black bars) or a scrambled control (open bars). Data is pooled from 5 separate experiments and depicted as relative luminescence compared to no-RNA controls (grey bars). Bars not connected by the same letters are statistically significantly different.

(D) Representative Western Blot analysis of RAW264.7 cells 12h post transfection with a mimic (pre-378) or inhibitor (anti-378) of miR-378-3p or appropriate negative controls (pre- & anti-neg). Samples were separated on 4-12% Bis-Tris gels and stained for Akt-1 and β-actin at the same time.

(E) Densitometric analysis of the samples analysed in (D). Data is representative of four separate experiments. Columns not connected by the same letters are statistically significantly different.

Figure 4: Akt-inhibition modulates alternative activation of MΦ *in vitro*.

(A) Thio-MΦ were stimulated with rIL-4 (+) or medium (-) following pre-incubation with the indicated concentration of triciribine for 1 hour and analysed for expression of alternative activation markers by qRT-PCR. Data is representative of three to four animals per group. Error bars indicate SEM. One of four experiments shown. Stars indicate statistical differences compared to IL-4 treated samples. *** $P < .001$, ** $P < .01$.

Figure 5: Timecourse of miR-378-3p expression and markers of proliferation following B.malayi implant.

(A) Gene expression of miR-378-3p and Akt1 in peritoneal MΦ isolated from *B. malayi* implanted C57BL/6 mice at the indicated timepoints post implant. N: naïve animals. Data points represent individual animals or separate pools of animals.

(B) FACS-analysis of Ki67 expression and BrdU-incorporation in the MΦ analysed in A.

Data from the same experiment shown in Jenkins et al[20(fig. S4)]

One experiment of one shown. *** $P < .001$; ** $P < .01$; * $P < .05$.

Figure 6: Akt-inhibition and miR-378-3p overexpression negatively regulate MΦ proliferation.

(A) BALB/c mice were injected i.p. with a single dose of triciribine (1 mg/kg) or vehicle control 1 hour prior to injection of IL-4c or PBS. 24 hours later cells were analysed for proliferation and alternative activation by FACS analysis. Each datapoint is representative of an individual animal. Pooled data from three separate experiments shown.

(B) Conversion of alamarBlue® by RAW264.7 cells 24h and 48h post transfection with a miR-378-3p mimic (black squares) or –inhibitor (black circles) or the appropriate negative controls (open symbols). Data representative of three separate experiments.

(C) FACS-analysis of Vybrant® CFDA SE dilution in the cells analysed in A.

(D) Gene expression of miR-378-3p target genes and genes associated with cell proliferation in RAW264.7 cells 48h post transfection with a miR-378-3p mimic (black bars) or the appropriate negative control (open bars).

*** $P < .001$; ** $P < .01$; * $P < .05$; n.s.: not significant

Figure 7: Induction of miR-378-3p is specific to IL-4 mediated signaling in MΦ.

(A) Thioglycollate-elicited, adherence-purified MΦ were incubated with rIL-4 (black squares), rM-CSF (grey circles) or with medium alone (open rectangles) for the indicated time and analysed for mi-RNA and mRNA-expression. Statistics indicate differences

between rM-CSF-treated samples and rIL-4-controls. *** $P < .001$. Each data point represents mean and SEM of six individual animals. Results from a single experiment shown.

(B) CD11b+F4/80+ (MΦ), CD19+F4/80- (B-cells), CD4+CD11b- lymphocytes (CD4+) and CD8+CD11b- lymphocytes (CD8+) were FACS-sorted from IL-4c injected (filled bars) or PBS injected control animals (open bars) and subjected to qRT-PCR. Data is depicted as fold change above PBS controls. Statistics indicate differences between IL-4c-treated samples and PBS-controls. *** $P < .001$; * $P < .05$. Bars depict mean and SEM of ten individual animals per group pooled from two independent experiments, except for the CD8+ data which is from one representative experiment. The second experiment is not shown because Ccna2 in the PBS controls was not detectable resulting in a fold change of infinity for the IL-4c treatment.

Figure 1

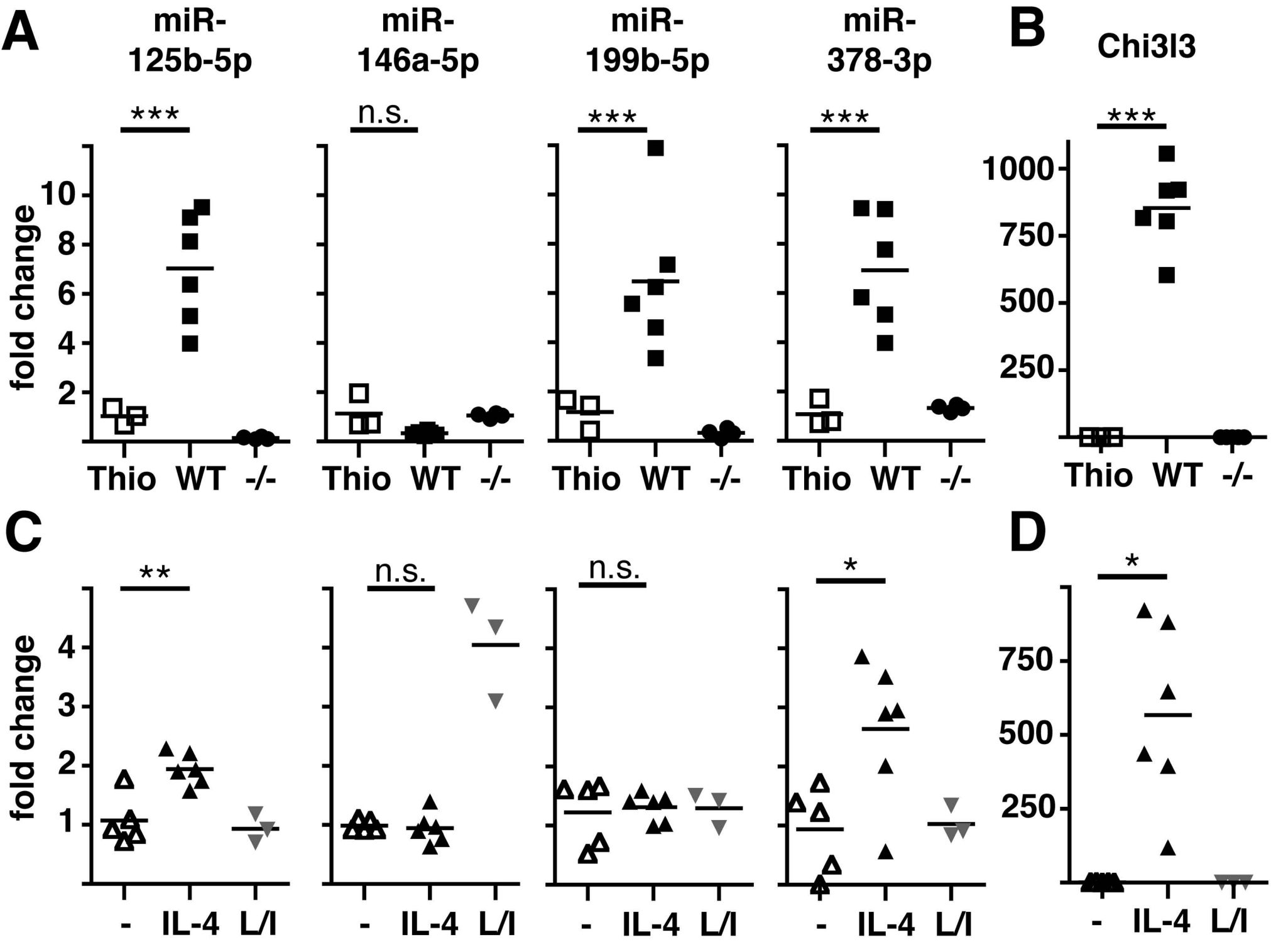
A
miR-125b-5p
miR-146a-5p
miR-199b-5p
miR-378-3p
***
n.s.
***
***
fold change
10
8
6
4
2
Thio
WT
-/-
B
Chi3l3
***
1000
750
500
250
C
**
n.s.
n.s.
*
fold change
4
3
2
1
-
IL-4
L/I
D
*
750
500
250

Figure 2

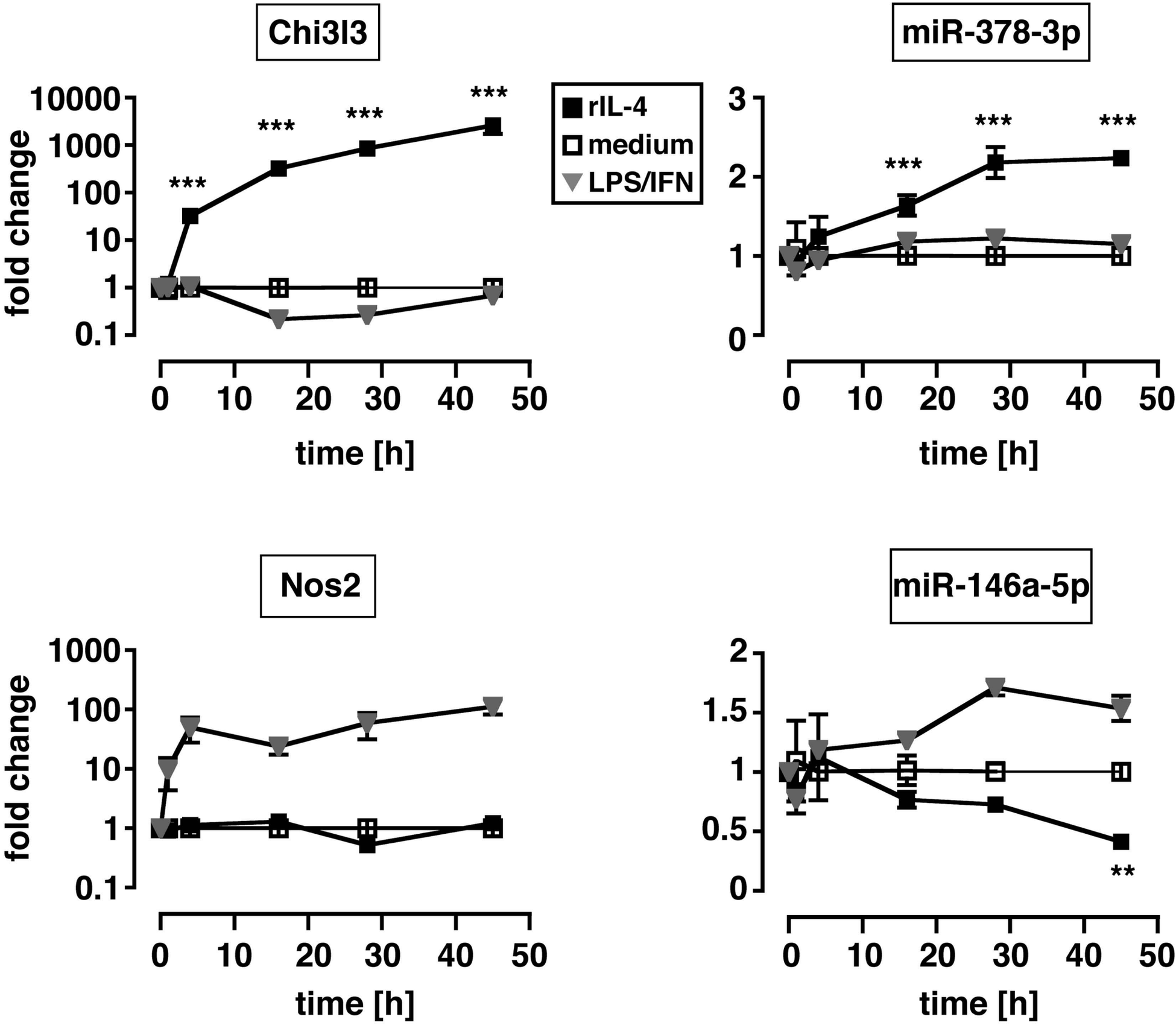

Figure 3

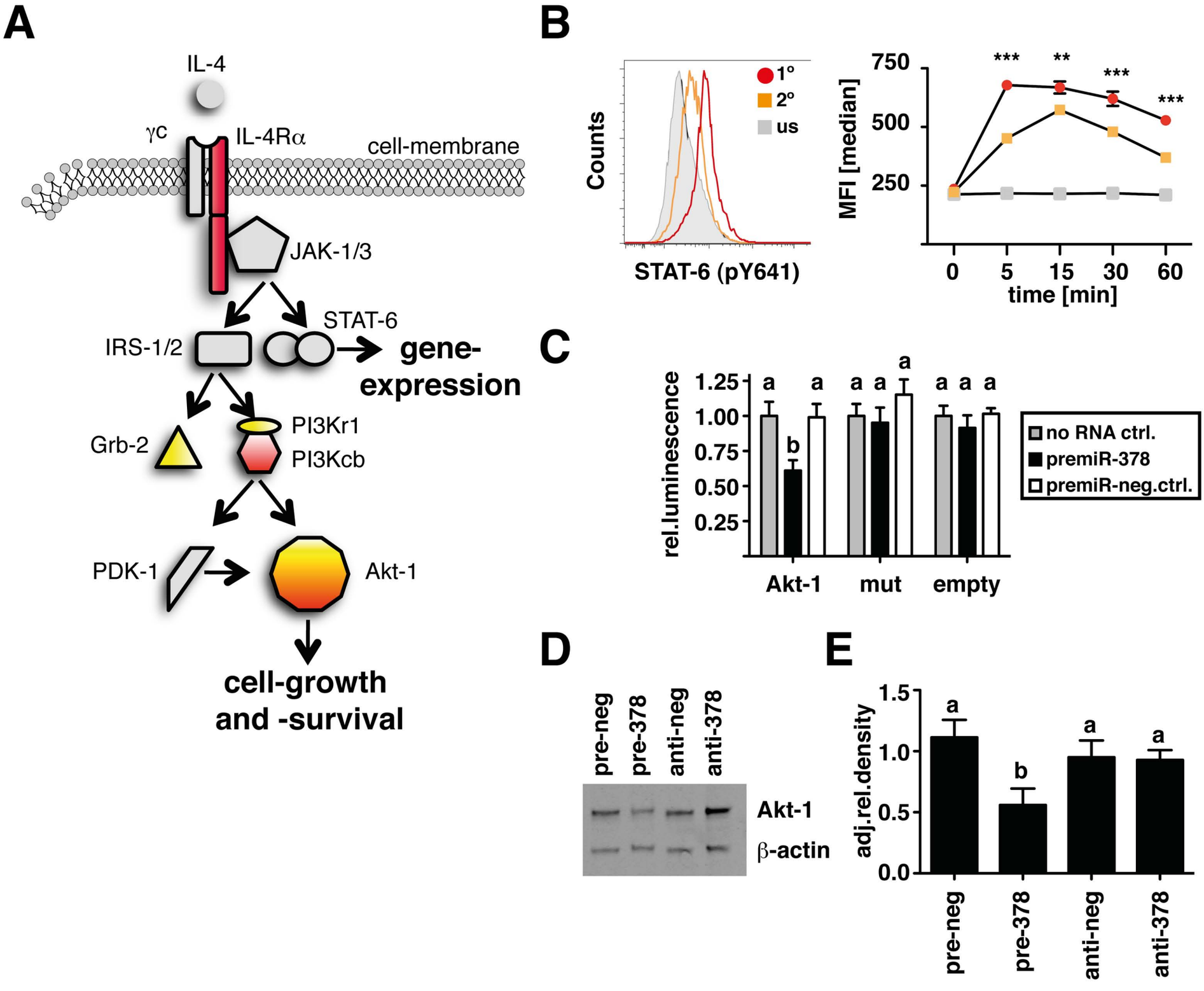
A
IL-4
γc
IL-4Rα
cell-membrane
JAK-1/3
STAT-6
IRS-1/2
gene-
expression
PI3Kr1
Grb-2
PI3Kcb
PDK-1
Akt-1
cell-growth
and -survival
B
Counts
1°
2°
us
STAT-6 (pY641)
MFI [median]
750
500
250
***
**
***
***
0
5
15
30
60
time [min]
C
rel.luminescence
1.25
1.00
0.75
0.50
0.25
a
b
a
a
a
a
a
a
a
Akt-1
mut
empty
no RNA ctrl.
premiR-378
premiR-neg.ctrl.
D
pre-neg
pre-378
anti-neg
anti-378
Akt-1
β-actin
E
adj.rel.density
1.5
1.0
0.5
0.0
a
b
a
a
pre-neg
pre-378
anti-neg
anti-378

Figure 4

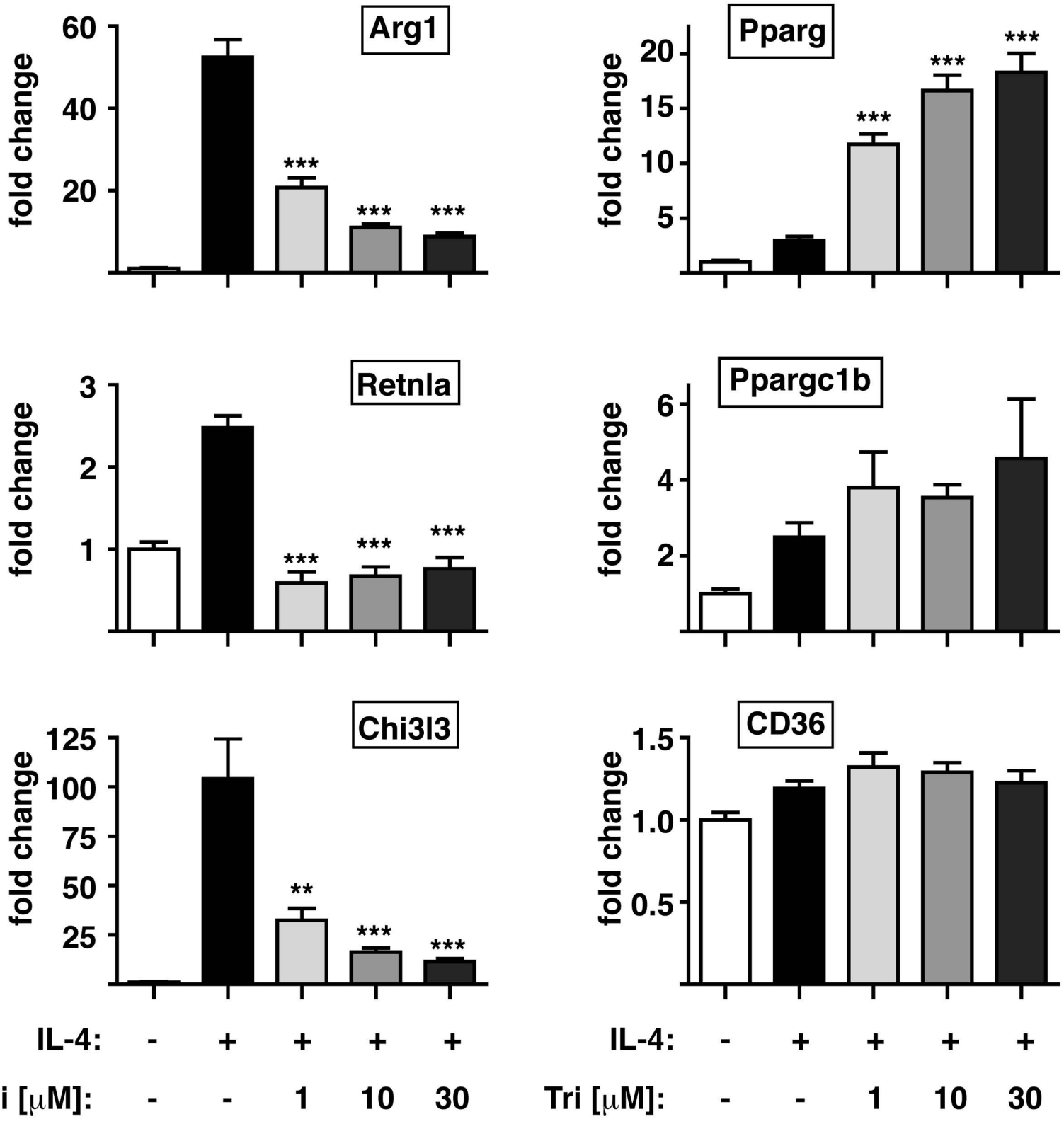
Arg1
fold change
60
40
20
***
***
***
Pparg
fold change
20
15
10
5
***
***
***
Retnla
fold change
3
2
1
***
***
***
Ppargc1b
fold change
6
4
2
Chi3l3
fold change
125
100
75
50
25
**
***
***
CD36
fold change
1.5
1.0
0.5
IL-4: - + + + +
Tri [μM]: - - 1 10 30
IL-4: - + + + +
Tri [μM]: - - 1 10 30

Figure 5

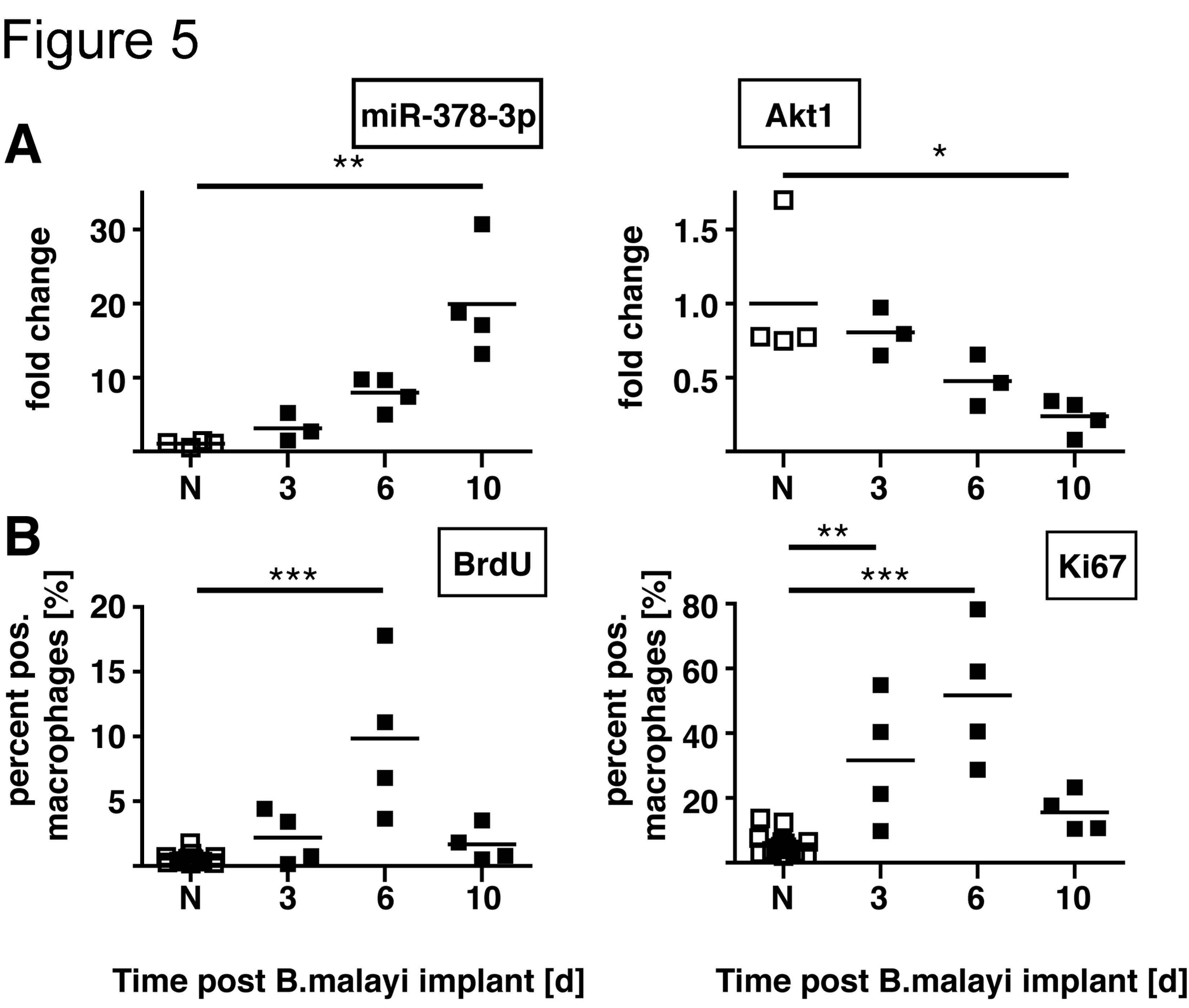
A
miR-378-3p
**
fold change
30
20
10
N
3
6
10
Akt1
*
fold change
1.5
1.0
0.5
N
3
6
10
B
BrdU
***
percent pos. macrophages [%]
20
15
10
5
N
3
6
10
Time post B.malayi implant [d]
Ki67
**
***
percent pos. macrophages [%]
80
60
40
20
N
3
6
10
Time post B.malayi implant [d]

Figure 6

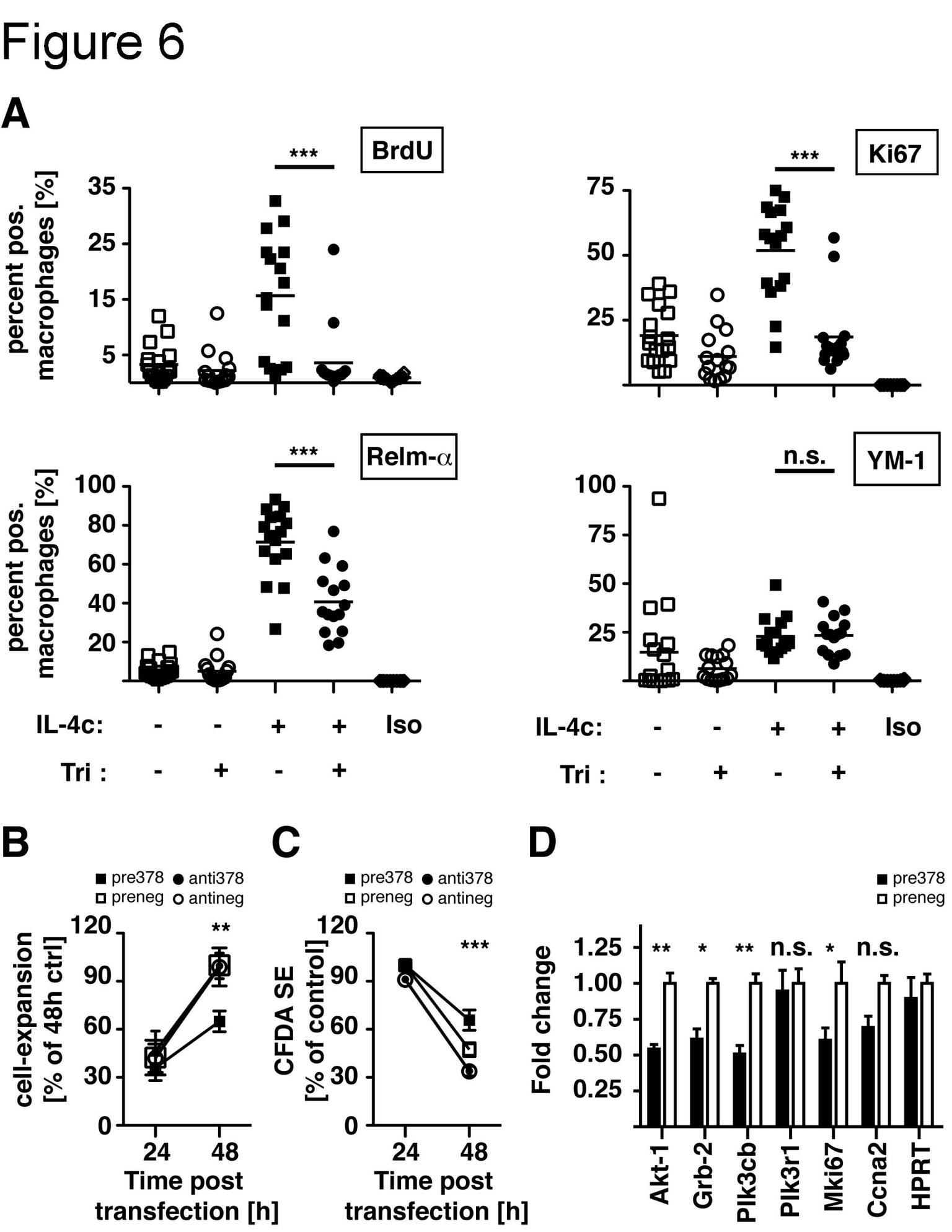
A
BrdU
***
percent pos. macrophages [%]
35
25
15
5
Ki67
***
75
50
25
Relm-α
***
100
80
60
40
20
YM-1
n.s.
100
75
50
25
IL-4c: - - + + Iso
Tri : - + - +
IL-4c: - - + + Iso
Tri : - + - +
B
pre378
anti378
preneg
antineg
cell-expansion [% of 48h ctrl]
120
90
60
30
0
**
24
48
Time post transfection [h]
C
pre378
anti378
preneg
antineg
CFDA SE [% of control]
120
90
60
30
0
***
24
48
Time post transfection [h]
D
pre378
preneg
Fold change
1.25
1.00
0.75
0.50
0.25
** * ** n.s. * n.s.
Akt-1
Grb-2
Plk3cb
Plk3r1
Mki67
Ccna2
HPRT

Figure 7